

# Towards efficient implementation of hybrid equilibrium plate elements

Edward Maunder\*, Angus Ramsay

\*Department of Engineering, University of Exeter  
Harrison Building, North Park Road, Exeter EX4 4QF, England  
e.a.w.maunder@exeter.ac.uk

## Abstract

This paper summarises the formulation of a hybrid equilibrium plate element based on semi-continuous fields of internal stresses and edge displacements which has the capability to produce statically admissible fields of stress-resultants. Implementation issues are discussed and advantage taken of the triangular shape of the constitutive primitive elements. An example of a plate with membrane actions is included to illustrate possibilities for  $p$ -type convergence.

## 1 Introduction

Finite element models composed of hybrid equilibrium elements have seen an upsurge in development due to the continued concern about the quality of results from computational methods and verification of their results. The role of equilibrium models to complement more conventional conforming displacement models has thereby been established. However their practical use has been called into question by Stein et al [7].

This paper summarises recent work to improve the efficiency of implementation of an hybrid equilibrium quadrilateral plate element for the simulation of elastic behaviour with small or large displacements. The element is formulated for a stiffness method of analysis so that it can be incorporated into new or existing software based upon this method. The main procedures of concern are: (a) the formation of a stiffness matrix of a macro-element composed from 4 primitive triangular elements (Maunder et al. [4,5]); (b) the inclusion of distributed loads when the current configuration of an element may change due to non-linear geometric effects; (c) the recovery of stress-resultants within an element.

The use of efficient algorithms means that characteristic matrices which are needed for various operations in a complete analysis may be reformed as and when required rather than being formed once and stored in memory. An example of the use of this element is included to illustrate  $p$ -type convergence.

## 2 Formulation

The formulation of the macro-element begins with triangular primitive elements as the “building blocks”. These are defined with continuous polynomial fields of statically admissible stress-resultants  $s$  and edge displacement fields  $d$  (appropriate for Reissner-Mindlin theory for plate bending) which are continuous for each edge but are

generally discontinuous for the boundary of the primitive. The basic equations for the primitive are summarised in Equation (1).

$$\mathbf{s} = \mathbf{S}\mathbf{s} + \mathbf{s}_p, \quad \mathbf{e} = \mathbf{f}\mathbf{s}, \quad \mathbf{t} = \bar{\mathbf{S}}\mathbf{s}, \quad \text{and} \quad \mathbf{d} = \mathbf{V}\mathbf{v} \quad (1)$$

where  $\mathbf{s}$  and  $\mathbf{v}$  denote stress and displacement parameters, subscript  $p$  denotes a particular solution equilibrating with a distributed load,  $\mathbf{t}$  denotes edge tractions equilibrating with  $\mathbf{s} = \mathbf{S}\mathbf{s}$ , and  $\mathbf{f}$  denotes the constitutive relations. These quantities are related by integral equations in Equation (2) which represent weak forms of compatibility and equilibrium respectively.

$$\int_D \mathbf{S}^T (\mathbf{f}\mathbf{S}\mathbf{s} + \mathbf{f}\mathbf{s}_p) dD = \int_G \bar{\mathbf{S}}^T \mathbf{d} \cdot dG \Rightarrow \mathbf{F}\mathbf{s} + \mathbf{d}_p = \mathbf{D}^T \mathbf{v} \quad \oint_G \mathbf{V}^T (\mathbf{t} + \bar{\mathbf{S}}_p) dG = \oint_G \mathbf{V}^T \bar{\mathbf{t}} \times dG \quad \mathbf{D}\mathbf{s} + \mathbf{g}_p = \bar{\mathbf{g}} \quad (2)$$

where  $\bar{\mathbf{S}}_p$  and  $\bar{\mathbf{t}}$  represent tractions which equilibrate with the particular solution and tractions which are prescribed or reactive respectively, and  $D$  and  $G$  denote the domain and boundary of the primitive. The characteristic matrices  $\mathbf{F}$  and  $\mathbf{D}$  are termed the natural flexibility matrix and the (boundary) work matrix. Further details of the static and kinematic characteristics will appear in Maunder et al. [6]. Elimination of  $\mathbf{s}$  leads to the stiffness form of element equations in Equation (3).

$$\mathbf{K}\mathbf{v} = \bar{\mathbf{g}} + (\mathbf{D}\mathbf{F}^{-1}\mathbf{d}_p - \mathbf{g}_p) \quad \text{where} \quad \mathbf{K} = \mathbf{D}\mathbf{F}^{-1}\mathbf{D}^T \quad (3)$$

The stiffness equations for the macro-element are first assembled as for a patch of elements in Equation (4).

$$\begin{array}{c|c} \hat{\mathbf{e}} \mathbf{K}_{ii} & \mathbf{K}_{ie} \hat{\mathbf{u}}_i \mathbf{v}_i \hat{\mathbf{u}}_i \\ \hline \hat{\mathbf{e}} \mathbf{K}_{ie}^T & \mathbf{K}_{ee} \hat{\mathbf{u}}_e \mathbf{v}_e \hat{\mathbf{u}}_e \end{array} = \begin{array}{c} \hat{\mathbf{e}} \mathbf{g}_i \hat{\mathbf{u}}_i \\ \hat{\mathbf{e}} \mathbf{g}_e \hat{\mathbf{u}}_e \end{array} \quad (4)$$

where suffices  $i$  and  $e$  denote internal and external edges respectively. Elimination of the internal freedoms leads to the condensed form of stiffness equations for the macro-element in Equation (5).

$$\mathbf{K}_{macro} \mathbf{v}_e \quad \circ \quad \left[ \mathbf{K}_{ee} - \mathbf{K}_{ie}^T \mathbf{K}_{ii}^+ \mathbf{K}_{ie} \right] \left\{ \mathbf{v}_e \right\} = \mathbf{g}_e - \mathbf{K}_{ie}^T \mathbf{K}_{ii}^+ \mathbf{g}_i \quad (5)$$

where the superscript + denotes the pseudo-inverse when  $\mathbf{K}_{ii}$  is singular due to the presence of spurious kinematic modes (Maunder et al. [4]). The right hand side of Equation (5) contains terms  $\mathbf{d}_p$  and  $\mathbf{g}_p$  associated with each primitive which represent distributed loading applied over the macro-element. The analysis of distributed loading can be considered in 3 stages: in stage 1 each primitive is analysed for reactive tractions corresponding to fixed edges, in stage 2 the internal edges of a macro are freed to obtain reactive tractions on the external edges, in stage 3 the external tractions are reversed and applied as statically equivalent edge loads to the complete assembly of macro-elements. In effect this multi-stage process transforms the initial particular solutions  $\mathbf{s}_p$  into one which satisfies the weak compatibility equations within each macro when its external edges are fixed. The final solution in terms of fields of stress-resultants is recovered by combining the particular solutions with those due to the displacements of all edges.

### 3 Implementation

The computations involved with the formulation have been organised to take advantage of special forms associated with the triangular shapes of the primitives, e.g. area coordinates and triangular stress components. Similar advantages have been recognised before, e.g. in the work of Argyris [1], but as far as the author is aware not in the context of hybrid equilibrium elements. Such forms are illustrated in Figure 1, where node 3 and edges of length  $a$  and  $b$  are internal to the macro and nodes 1 and 2 as well as edge of length  $c$  are external. Note that the corner nodes are only required as geometric entities for primitives with straight edges. Oblique axes  $x, y$  have their origin at node 3, area coordinates are denoted by  $L_1, L_2$ , and  $L_3$ .

Triangular components of stress-resultants are indicated in Figure 1 as intensities of actions on the edges of an infinitesimal triangle of similar shape and orientation to the primitive. Membrane force and moment fields, when shear forces are excluded, form columns of  $\mathbf{S}$  and are generated from Airy stress functions  $\mathbf{F}$  using the first part of Equation (6) where  $\mathbf{s}$  denotes  $n$  or  $m$ . The remaining moment fields in  $\mathbf{S}$  are generated from shear force fields derived from a first order stress function  $\mathbf{W}$  (Fraeijs de Veubeke [3]) in the second part of Equation (6). Oblique

components of moments  $m_x$  and  $m_y$  are derived by indirect integration of oblique shear force components with the assumption that torsional moments are zero. These components are then transformed into triangular components.

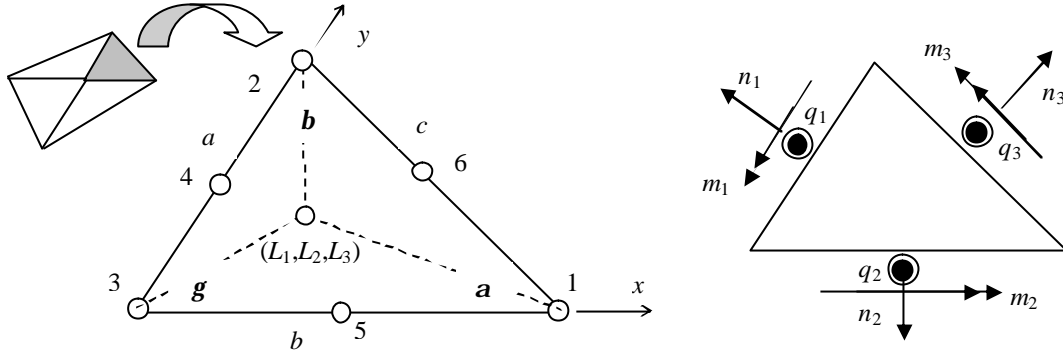


Figure 1: primitive element, local axes and coordinates; triangular stress components.

$$\begin{matrix} \dot{\mathbf{S}}_1 \\ \dot{\mathbf{S}}_2 \\ \dot{\mathbf{S}}_3 \end{matrix} \begin{matrix} \ddot{\mathbf{u}} \\ \ddot{\mathbf{y}} \\ \ddot{\mathbf{p}} \end{matrix} = \begin{matrix} \hat{\mathbf{e}} \\ \hat{\mathbf{e}} \\ \hat{\mathbf{e}} \end{matrix} \begin{matrix} \frac{1}{a^2} & 0 & 0 \\ 0 & \frac{1}{b^2} & 0 \\ 0 & 0 & \frac{1}{c^2} \end{matrix} \begin{matrix} \ddot{\mathbf{u}}_1 \\ \ddot{\mathbf{u}}_2 \\ \ddot{\mathbf{u}}_3 \end{matrix} - 2 \begin{matrix} \frac{\mathbb{1}^2}{\mathbb{L}_2 \mathbb{L}_3} \\ \frac{\mathbb{1}^2}{\mathbb{L}_1 \mathbb{L}_3} \\ \frac{\mathbb{1}^2}{\mathbb{L}_1 \mathbb{L}_2} \end{matrix} + \begin{matrix} \frac{\mathbb{1}^2}{\mathbb{L}_3} \\ \frac{\mathbb{1}^2}{\mathbb{L}_2} \\ \frac{\mathbb{1}^2}{\mathbb{L}_1} \end{matrix} \begin{matrix} \ddot{\mathbf{u}} \\ \ddot{\mathbf{y}} \\ \ddot{\mathbf{p}} \end{matrix} \mathbf{F} ; \quad \begin{matrix} \dot{\mathbf{q}}_1 \\ \dot{\mathbf{q}}_2 \\ \dot{\mathbf{q}}_3 \end{matrix} \begin{matrix} \ddot{\mathbf{u}} \\ \ddot{\mathbf{y}} \\ \ddot{\mathbf{p}} \end{matrix} = \begin{matrix} \hat{\mathbf{e}} \\ \hat{\mathbf{e}} \\ \hat{\mathbf{e}} \end{matrix} \begin{matrix} -1/a & 0 & 0 \\ 0 & -1/b & 0 \\ 0 & 0 & 1/c \end{matrix} \begin{matrix} \ddot{\mathbf{u}}_1 \\ \ddot{\mathbf{u}}_2 \\ \ddot{\mathbf{u}}_3 \end{matrix} - \begin{matrix} \frac{\mathbb{1}}{\mathbb{L}_2} \\ \frac{\mathbb{1}}{\mathbb{L}_3} \\ \frac{\mathbb{1}}{\mathbb{L}_1} \end{matrix} \begin{matrix} \ddot{\mathbf{u}} \\ \ddot{\mathbf{y}} \\ \ddot{\mathbf{p}} \end{matrix} \mathbf{W} \quad (6)$$

The compliance matrix  $f$  is formed as  $\mathcal{P}$  to correspond to triangular components of force and moment stress-resultants.  $\mathbf{F}$  is constructed using a hierarchical sequence for ordering the columns of  $\mathbf{S}$ , e.g. for bending actions the first 3 columns correspond to constant moment fields, the next 6 correspond to linear moment fields with the first set of 4 having no shear forces and the second set of 2 having shear forces, etc for increasing degrees of the fields. Coefficients of  $\mathbf{F}$  are evaluated using exact integration formulae for simple products of area coordinates (Burnett [2]). This is conveniently organised using scalar products of matrices which includes a matrix  $\mathbf{M}$  of integrals of products of interpolation functions  $N_r$  and  $N_s$ , e.g. contributions from moment fields are evaluated as in Equation (7).

$$\mathbf{F}_{ij} = [\mathbf{M}] \cdot [\tilde{\mathbf{m}}_i^T \mathbf{f}_m^D \tilde{\mathbf{m}}_j] \quad \text{with} \quad \int_D N_r N_s dD = \mathbf{M}_{rs} \in [\mathbf{M}] \quad (7)$$

where for example the  $3 \times n_i$  matrix  $\tilde{\mathbf{m}}_i$  contains the components of the  $i^{\text{th}}$  moment field at  $n_i$  reference points (nodes),  $n_i$  being the number of interpolation functions required to define the field.

The algebraic forms of edge traction distributions corresponding to the columns of  $\bar{\mathbf{S}}$  in  $\mathbf{D} = \oint_G \bar{\mathbf{V}}^T \bar{\mathbf{S}} dG$  lead to

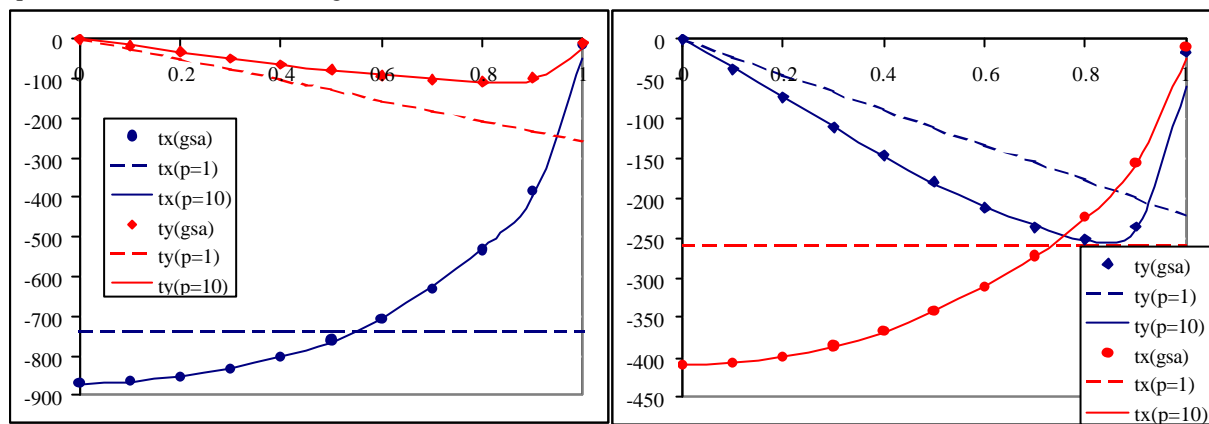
traction modes whose amplitudes represent edge resultant forces and/or moments for distributions of low degree, or self-balancing modes for distributions of higher degree. Using dual bases for traction and displacement modes, the coefficients of  $\mathbf{D}$  are thus formed directly by scalar products as simple algebraic expressions.

Distributed loading is accounted for by using a single continuous particular solution  $\mathbf{s}_p$  over the whole macro. This simplifies stage 2 since terms involving  $\mathbf{g}_p$  cancel out along internal edges. If, furthermore,  $\mathbf{s}_p$  is defined as a Trefftz field, then terms involving the vectors  $\mathbf{d}_p$  can be evaluated as scalar products of edge traction modes equilibrating with the columns of  $\mathbf{S}$  and displacement modes derived from the Trefftz fields of stress-resultants.

The construction of the stiffness matrix in Equation (5) involves a singular matrix  $\mathbf{K}_{ii}$  when the macro is formed by diagonal subdivision of a quadrilateral. A simpler alternative to forming a pseudo-inverse by singular value decomposition is possible since the spurious kinematic mode is known explicitly. In this case the dimensions of the vector  $\mathbf{v}_i$  and the matrices  $\mathbf{K}_{ii}$  and  $\mathbf{K}_{ie}$  can be reduced by selecting a smaller basis for  $\mathbf{v}_i$  which excludes the spurious kinematic mode.

#### 4 An example to illustrate $p$ -convergence

A simple numerical example illustrates the solution for reactive tractions for a 2m square plate subjected to an in-plane UDL = 1 kN/m<sup>2</sup> in a direction parallel to an edge, the  $x$ -axis, giving a total load of 4kN. The plate has unit thickness and a Poisson's ratio of 0.3 with fixed edges. A single macro-element with diagonal subdivision is used to model the top right quadrant of the plate. Reaction components are shown in Figure 2 with normal tractions in blue and tangential tractions in red. Dashed lines indicate the solution for stress fields of unit degree, whilst continuous lines indicate the solution for stress fields of degree 10. The solutions are compared with that from a conventional conforming finite element model denoted by (gsa) based on a uniform mesh of 8-noded quadrilateral elements with edge dimension 0.05m.



Reactive tractions in kN/m<sup>2</sup> on the right hand edge      Reactive tractions in kN/m<sup>2</sup> on the top edge  
Figure 2: Distributions of tractions on the fixed edges of a square plate.

The edge tractions show excellent agreement with those from the refined conforming model, except in the neighbourhood of the corners where large stress gradients exist which should lead to zero stress states at the corner points. However it must be remembered that the hybrid tractions are in complete equilibrium with the loads and the internal stresses so that upper bounds for global errors can be determined.

It is intended to incorporate hybrid plate elements of general degree into software based on stiffness methods using generalised static and kinematic edge variables referenced to midside nodes, with curved edges to model the boundary of the model domain. It is also intended to explore the potential benefits of such elements.

#### References

- [1] Argyris J, Tenek L. Natural mode method: A practicable and novel approach to the global analysis of laminated composite plates and shells. *Applied Mechanics Reviews* 1996; **49**: 381-399.
- [2] Burnett DS. *Finite Element Analysis*. Addison-Wesley, Reading, Massachusetts, 1987.
- [3] Fraeijs de Veubeke BM. Stress function approach. In *B.M. Fraeijs de Veubeke Memorial Volume of Selected Papers*, Geradin M (ed). Sijthoff & Noordhoff: Alphen aan den Rijn, 1980; 663-715.
- [4] Maunder EAW, Moitinho de Almeida JP, Ramsay ACA. A general formulation of equilibrium macro-elements with control of spurious kinematic modes: the exorcism of an old curse. *International Journal for Numerical Methods in Engineering* 1996; **39**: 3175-3194.
- [5] Maunder EAW. Hybrid elements in the modeling of plates. In *Finite Elements: Techniques and Developments*, Topping BHV (ed). Civil-Comp Press: Edinburgh, 2000; 165-172.
- [6] Maunder EAW, Moitinho de Almeida JP. A Triangular Hybrid Equilibrium Element of General Degree. Accepted 2004 for publication in *International Journal for Numerical Methods in Engineering*.
- [7] Stein E, Ruter M. Finite Element Methods for Elasticity with Error-controlled Discretization and Model Adaptivity. Chapter 2 in *Encyclopedia of Computational Mechanics, Volume 2, Solids and Structures*, Stein E, de Borst R, Hughes TJR (eds). Wiley: Chichester, 2004; 5-58.